Contrib. Mineral. Petrol. 72, 243-255 (1980)

Contributions to Mineralogy and Petrology

Mineralogy, Petrology, and Phase Relations of Glaucophane-Lawsonite Zone Blueschists From the Tavşanlı Region, Northwest Turkey

A.I. Okay

Department of Mineralogy and Petrology, Downing Place, Cambridge CB2 3EW, England

Abstract. Glaucophane-lawsonite facies blueschists representing a metamorphosed sequence of basic igneous rocks, cherts and shales have been investigated northeast of the district of Tavşanli in Northwest Turkey. Sodic amphiboles are rich in magnesium reflecting the generally high oxidation states of the blueschists. Lawsonite has a very uniform composition with up to 2.5 wt.% Fe_2O_3. Sodic pyroxenes show an extensive range of compositions with all the end-members represented. Chlorites are uniform in their Al/(Al+Fe+Mg) ratio but show variable Fe/(Fe+Mg) ratios. Garnets from metacherts are rich in spessartine (>50%) whereas those from metabasites are largely almandine. Pistacite rich epidote is found in metacherts coexisting with lawsonite. Phengites are distinctly higher in their Fe, Mg and Si contents than those from greenschist facies. Hematites with low TiO_2 are ubiquitous in metacherts.

Fe^{2+}/Mg partitioning between chlorite and sodic amphibole is strongly controlled by the calcium content of the sodic amphibole and ranges from 1.1 for low calcium substitution to 0.8 for higher calcium substitution. The Al/Fe^{3+} partition coefficient between sodic amphibole and sodic pyroxene is 2.1.

A model system has been constructed involving projections from lawsonite, iron-oxide and quartz onto a tetrahedron with Na, Al, Fe^{2+} and Mg at its apices. Calcite is treated as an indifferent phase. The model system illustrates the incompatibility of the sodic pyroxene with chlorite in the glaucophane-lawsonite facies; this assemblage is represented by sodic amphibole.

Sodic amphibole compositions are plotted in terms of coexisting ferromagnesian minerals. Five major areas on the sodic amphibole compositional field are delineated, each associated with one of the following minerals: chlorite, stilpnomelane, talc, almandine, deerite.

Introduction

In Northwest Turkey blueschists form a coherent, discontinously exposed metamorphic belt about 20 km in width and 300 km in length (Fig. 1, inset). They flank the northern margins of the large ultramafic massifs in the eastern part of the İzmir-Ankara ophiolite zone (Brinkmann 1972) forming a regionally metamorphosed eugeosynclinal sequence of basic volcanic rocks, cherts, shales and minor gabbroic intrusions.

Although the existence of blueschists in Turkey have been known for over seventy years (cf. van der Kaaden 1966), the first detailed study on their petrology was not published until 1967 by Çoğulu. He worked in the eastern part of the Northwest Turkish blueschist belt in the region of Mihalliçik, and distinguished three metamorphic zones: lawsonite, lawsonite-crossite, and epidote-crossite with an increase in grade northwards. He also obtained ages for blueschist metamorphism of 60–80 Ma (Çoğulu and Krummenacher 1967). Lünel (1967) studied a small area of glaucophane-lawsonite facies blueschists south of Eskisehir (Fig. 1, inset) with special reference to the bulk rock chemistry and structure. Kaya (1972) worked on the isolated small blueschist outcrops south of Tavşanlı.

Geology

Throughout the NW Turkish blueschist/ultramafic belt the outcrops are separated by an extensive Neogene cover. A large area (20 to 45 km) of blueschists, ultramafics and marbles protrudes from under the Neogene northeast of the district of Tavşanlı (Fig. 1, inset). During the course of the present study, part of this extensive area (30 to 13 km) of blueschists and ultramafics was mapped in detail and over 700 rock specimens were collected for petrological investigations. In the studied area glaucophane-lawsonite zone blueschists form a coherent, complexly deformed regional

0010-7999/80/0072/0243/$02.60

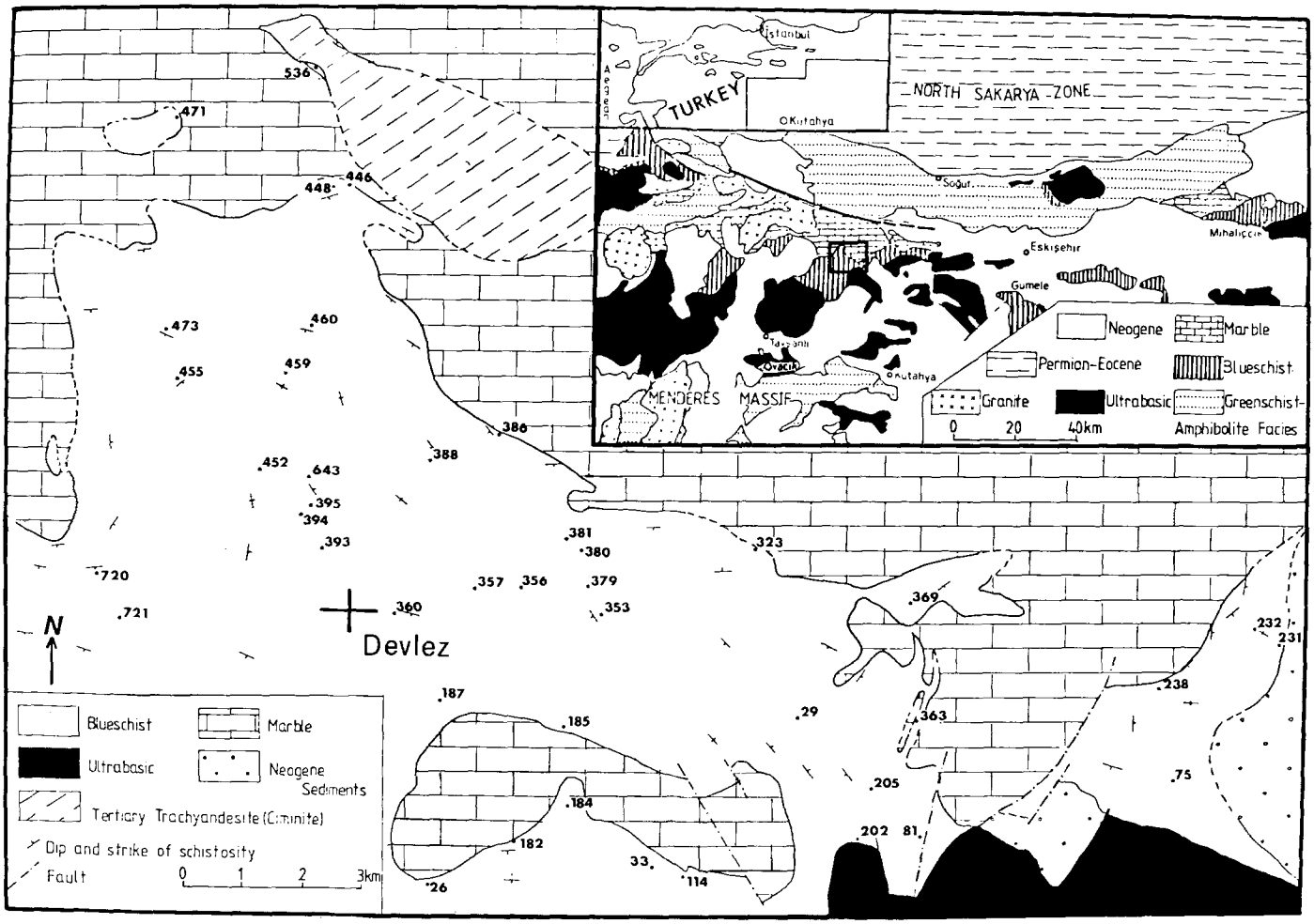

Fig. 1. Simplified geological map of Devlez area, Northeast Tavşanlı. Locations of analysed specimens and specimen numbers are indicated. The inset shows a simplified and generalized geotectonic map of Northwest Turkey, compiled from the geological maps of Northwest Turkey (Maden Tetkik ve Arama Enst. 1963, 1964) and the author's own observations

metamorphic terrain. Towards the south they pass into an area of lawsonite-sodic pyroxene-chlorite rocks (Okay, in preparation). This narrow zone (2–3 km) is in tectonic contact with an incipiently metamorphosed spilite-chert-serpentinite complex and an ultrabasic massif.

This paper deals with the northern glaucophane-lawsonite zone blueschists in the vicinity of the village of Devlez which form a broad southerly-plunging synform, lying on a very thick, massive marble series (Fig. 1). Occasional calcite pseudomorphs after lawsonite in some impure marble beds indicate that at least part of the marbles have been metamorphosed in the blueschist facies.

No grade change across the region is detectable indicating relatively uniform metamorphic conditions over a fairly large area. The blueschists do not show any evidence of polymetamorphism and retrogressive readjustment has been very minor.

Rock Types

The blueschists form a monotonous, metamorphosed sequence of basic volcanic rocks interbedded with cherts and siliceous shales. Small metagabbroic lenses and manganese rich rocks occur in minor quantities (< 1% of the exposures). Metagreywackes, interbedded marbles and lenses of serpentinite have not been found in the blueschist terrain of Devlez. Occasional veins contain calcite and/or quartz.

Basic metavolcanic rocks make up approximately 50%–60% of the exposures. Most are completely recrystallized with a penetrative schistosity and with no traces of their previous igneous mineralogy and texture. The common mineral assemblages in the metabasites are:

sodic amphibole + lawsonite + phengite + sphene ± sodic pyroxene ± chlorite ± quartz.

Sodic amphibole and lawsonite are by far the most common phases in the metabasites, usually occurring in roughly equal amounts (35%–50% each) and together making up over 80% of the rock. Phengite and sphene are present in virtually all metabasites as minor components (1%–10% each). The modal amount of sodic pyroxene is quite variable ranging up 25%. Chlorite and quartz are found as minor phases making up to 15% of the mode. Other phases which may be present in the metabasites include calcite, aragonite, almandine garnet and magnetite. Measured modes of two typical metabasites based on over 2,000 point counts are given in Table 1.

Metacherts occur as thinly-bedded quartzites with black lineations due to the development of parallel oriented sodic amphibole prisms and hematite platelets (Fig. 2). Metashales tend to be rich

Table 1. Measured modes of typical

	Metabasites		Metachert	Metashale
	K33 (279)	K643/2 (326)	K460 (366)	K473 (367)
Sodic amphibole	45.4	36.6	9.8	4.5
Lawsonite	36.2	27.7	5.9	1.3
Sodic pyroxene	0.8	22.5	–	–
Chlorite	tr.	1.0	tr.	–
Garnet	–	–	5.2	0.3
Quartz	–	–	70.7	72.2
Carbonate	6.3 CA	–	–	–
Hematite	–	–	4.8	1.8
Magnetite	0.2	–	–	–
Pyrite	–	0.2	–	–
Phengite	5.0	2.9	3.6	19.3
Sphene	5.9	9.2	–	tr.
Tourmaline	0.2	–	–	tr.
Apatite	–	–	tr.	tr.

tr. < 0.1

The numbers in brackets preceded by 122 (e.g. 122279) are Harker specimen numbers. All specimens are kept in the Harker Collection in the Department of Mineralogy and Petrology in Cambridge. CA-aragonite retrograding to calcite

in white mica and consequently well-foliated with a silvery-white lustre. Both metacherts and metashales, henceforth referred to simply as metacherts, invariably have highly oxidised mineral assemblages with abundant hematite (Table 3 and Fig. 2). They make up 40%–50% of the exposures in the Tavşanli area. The most common mineral assemblages in metacherts are:

quartz + phengite + garnet + sodic amphibole + hematite + lawsonite ± epidote ± chlorite.

Quartz is the dominant phase in metacherts making up 70%–90% of the rock. Phengite is the next most abundant mineral

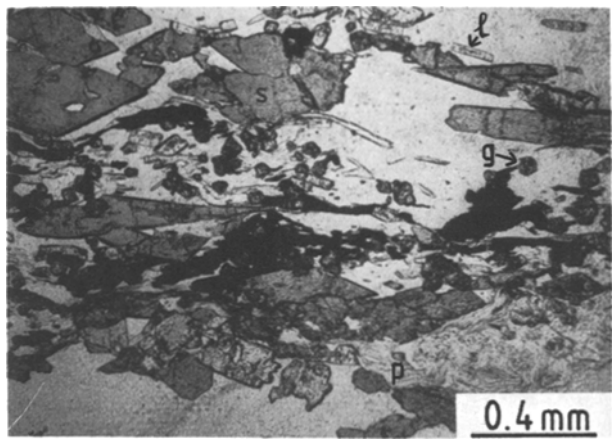

Fig. 2. Photomicrograph of a ferromagnesian-rich band in metachert (K460) illustrating garnet (*g*), lawsonite (*l*), hematite (*black*), crossite (*s*) and phengite (*p*) all set in quartz

forming 5%–10% of the mode. Garnet, sodic amphibole, hematite, lawsonite and epidote occur in variable quantities each forming 1% to 5% of the rock. Chlorite, where present, commonly makes up 1%–2%. Sodic pyroxene is occasionally found in some metacherts. Table 1 gives the measured modes of one metachert (s.s.) and one metashale.

Fine-grained, pale-green jadeite-quartz-lawsonite-phengite rocks with a granoblastic texture (?meta-keratophyres, Table 3) are found intercalated with the metabasites. Other rare rock types include, dark-green, silica-undersaturated aegerine-chlorite-lawsonite rocks and spessartine-braunite bearing meta-manganese deposits.

Method

Mineral compositions were determined for twelve elements (Na, Ca, K, Fe, Mg, Mn, V, Ni, Cr, Ti, Al, Si) using an electronprobe microanalyser with a Harwell Si(Li) detector and pulse processor

Table 2. Mineral assemblages in 19 analysed metabasites

	K26/1 (275)	K27 (276)	K29/1 (277)	K29/2 (386)	K75/1 (291)	K114 (295)	K185 (312)	K187 (313)	K231/3 (344)	K323 (350)	K356 (353)	K357/1 (320)	K363/1 (355)	K388 (360)	K394/1 (362)	K446/1 (322)	K455 (323)	K471 (324)	K536 (375)
Sodic amphibole	×	×	×	×	×	×	×	×	×	×	×	×	×	×	×	×	×	×	×
Lawsonite	×	×	×	×	×	×	×	×	×	×	×	×	×	×	×	×	×	×	×
Epidote								×								×	×		
Sodic pyroxene			×	×	×	×			×	×	×				×		×		
Chlorite	×	×	×	×	×						×		×		×			×	×
Garnet												×				×			
$CaCO_3$	×	×		×		×			×				×			×		×	×
Hematite						×		×	×					×					
Magnetite	×		×				×	×		×									
Quartz	×	×	×				×	×	×	×		×	×	×					×
Albite		×												×				×	
Phengite		×	×	×	×	×	×	×	×	×		×	×	×		×	×	×	×
Sphene	×	×	×	×	×	×	×			×		×	×	×		×	×	×	×
Others		1, 2									3, 4				3, 5	1			

1: apatite; 2: tourmaline; 3: relict augite; 4: talc; 5: pumpellyite

The numbers in brackets preceded by 122 (e.g. 122275) are Harker specimen numbers. All specimens are kept in the Harker Collection in the Department of Mineralogy and Petrology in Cambridge

Table 3. Mineral assemblages in 10 analysed metacherts and metashales, and 2 metakeratophyres

	K182 (310)	K184 (311)	K231/4 (345)	K232/1 (316)	K379 (356)	K380 (357)	K381 (358)	K448/1 (363)	K452 (364)	K459 (365)	K395 (385)	K721/1 (384)
Sodic amphibole	×	×	×	×	×	×	×	×	×	×		
Lawsonite			×	×	×	×		×	×	×	×	×
Epidote				×		×			×	×		
Sodic pyroxene	×	×					×				×	×
Chlorite	×		×					×				
Garnet	×	×	×	×	×	×		×	×	×		
Hematite	×		×	×	×	×		×		×		
Quartz	×	×	×	×	×	×	×	×	×	×	×	×
Phengite	×	×	×	×	×	×		×	×	×	×	
Sphene	×	×		×		×						
Apatite	×	×	×		×	×	×			×		

(Statham 1976). The correction procedures are given by Sweatman and Long (1969). To check the accuracy of the analyses an olivine standard supplemented by a jadeite standard was used throughout. The accuracy is estimated to be 2% for major elements (more than 5% element present). The method for estimating ferric ion in sodic pyroxene and sodic amphibole is given in earlier papers (Okay 1978, in press).

Mineralogy

Sodic Amphibole

One hundred sixty sodic amphibole analyses from 21 metabasites and 14 metacherts are plotted in the Miyashiro's (1957) diagram in Fig. 3 and eight of these are given in Table 4. The actinolite component in the analysed sodic amphiboles is usually small ($Ca/(Ca+Na)=X_{Ca}<0.1$). It is generally higher in sodic amphiboles from metabasites than those from the metacherts ($X_{Ca}<0.05$). No coexisting calcic and sodic amphibole pairs are found in the Devlez area.

Lawsonite

The composition of lawsonite is remarkably uniform and closely approximates to the ideal structural formula $CaAl_2Si_2O_7\text{-}H_2O(OH)_2$ with the only noticable substitution being Al by Fe (max. 2.5 wt.% Fe_2O_3).

Sodic Pyroxene

Sodic pyroxene is a common constituent of the metabasic rocks in the Devlez area. It occurs less commonly in the metacherts. In the metabasites, sodic pyroxene is found as xenoblastic grains showing occasional replacement by sodic amphibole. However, such textures are lacking in the metacherts where idioblastic equigranular sodic pyroxene and sodic amphibole grains coexist stably.

Seventy-five sodic pyroxene compositons from 18 samples from the Devlez area, including the eight previously published, are plotted in the acmite-jadeite-augite ternary diagram in Fig. 4; six of the analyses are given in Table 4. As noted in an earlier paper (Okay 1978) sodic pyroxenes from glaucophane-lawsonite facies metabasites tend to be enriched in the acmite component, compared with the sodic pyroxenes from eclogites and higher grade blueschists. Jadeite is found in some rare, massive metakeratophyres.

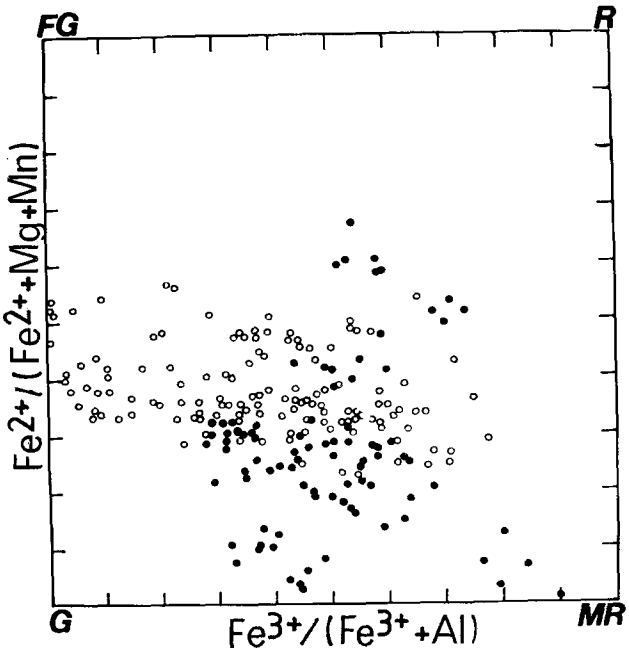

Fig. 3. Sodic amphibole compositions from Devlez area plotted on the Miyashiro diagram. Sodic amphiboles from metacherts, *filled circles*; from metabasites, *open circles*. *G* glaucophane; *FG* ferroglaucophane; *R* riebeckite; *MR* magnesioriebeckite

Chlorite

Small amounts of chlorite are found in about one third of the blueschist samples studies from the Devlez area. Chlorite is much rarer in metacherts only becoming a major phase in some rare, sodium-free or silica-undersaturated rocks.

Chlorites show a wide range of ferromagnesian ratios ($X_{Fe}=0.2$–0.6) and a restricted Al/(Al+Fe+Mg+Mn) ratio (0.29–0.34). Chlorite compositions are plotted in Fig. 5 and four chlorite analyses are shown in Table 4. Compared with the chlorites from the greenschist facies, where the Al/(Al+Fe+Mg+Mn) ratio ranges between 0.35 and 0.40 (Brown 1967; Cooper 1972), chlorites from blueschists are characterized by their higher silica and lower alumina contents (Fig. 5). The substitution involved is $Si(Fe^{2+}, Mg)=2Al$.

Garnet

The two major rock types in the Devlez area, namely metabasites and metacherts, contain chemically and texturally distinct types of garnet. Metacherts commonly have abundant small (< 0.1 mm) granular garnet grains associated with quartz, phengite, hematite and sodic amphibole (Fig. 2). These garnets tend to be rich in spessartine (> 50%) with very low values of pyrope (av. 1%). Garnets of this type are common in the Franciscan Complex (Ernst et al. 1970) and in New Caledonia (Black 1973).

The second and much rarer type of garnet is found in rocks of basic igneous composition. These tend to be much larger in size (1–3 mm) and more sporadic in occurrence than the first type. They consist dominantly of almandine-grossular components with lesser pyrope (8%–10%) and spessartine (1%–5%); and are similar in composition to the garnets from type III metabasites from the Cazadero area in California (Lee et al. 1963).

Garnets from 10 metacherts and 5 metabasites are plotted in Fig. 6 in terms of grossular, spessartine and almandine + pyrope end-members; six garnet analyses, three from metabasites and three from metacherts, are shown in Table 4. Garnets from the Devlez area show complete solid solution between almandine and spessartine.

Zoning in the spessartine-rich garnets from the metacherts is difficult to observe because of the very small size of the grains. However, analyses of separate garnet grains in a single thin section usually reveal variations in composition between 20–30 mol.% spessartine-almandine with a fairly constant grossularite content. The grossularite contents of all analysed spessartine garnets are relatively constant lying between 10–20 mol.% (Fig. 6). Only garnets from one metabasite out of five showed zoning involving an increase of almandine towards the rim (Fig. 6, Table 4).

Epidote

Epidote is a rare mineral in the area; it mainly occurs in some metacherts in association with hematite and lawsonite. Twenty-three epidotes from 4 metacherts and 3 metabasites were analysed and these are shown on a histogram in Fig. 7a. Epidotes from metacherts are invariably pistacite-rich (27%–35% pistacite), and occur in much less abundance than the accompanying lawsonite. In metabasites, epidote is usually found as small, rounded inclusions in lawsonite porphyroblasts, suggesting that it is a relict phase from a spilitic protolith. Epidotes from metabasites are less pistacite-rich than those from metacherts, with pistacite components of 20%–28%. All epidotes contain small amounts of Mn which substitutes for Ca.

The assemblage epidote-lawsonite-hematite, as found in two metacherts (Table 3), is compositionally invariant at constant P and T in the system $Ca-Al-Fe^{3+}$; neglecting small amount of Mn in epidote (0.07 per formula unit) and Ti in hematite (0.07 per formula unit). The pistacite component of the epidote and the ferric content of lawsonite must be a maximum for this invariant assemblage under the particular conditions of metamorphism (Fig. 7b). Epidotes from the two metacherts have very similar pistacite components (31% and 32%); the lawsonites have relatively high iron contents (av. 0.08 per formula unit) confirming the invariance of the subassemblage.

Phengite

Phengite is the only major K-bearing phase in the Devlez blueschists. It is an important consituent in the metacherts, and is common as a minor phase in metabasites. Sixty-two phengite analyses from 15 metabasites and 11 metacherts are shown in the Al–Fe–Mg diagram in Fig. 8, six of these are given in Table 4. The Devlez phengites are richer in Fe, Mg and Si than those of the greenschist facies (cf. Brown 1967). In those from the metabasites there is not even an overlap between the blueschist and greenschist compositions (Fig. 8). All analysed phengites show very limited solid solution towards Ca-mica (< 1 mol.%) and no solid solution with paragonite.

Hematite

Hematite is an essential part of the metachert mineral assemblage. It occurs as abundant, small platelets closely associated with the other ferromagnesian minerals in the rock (Fig. 2). Fourteen analysed hematites from 9 metacherts and 2 metabasites contain up to 4 wt.% TiO_2 and 0.2 wt.% V_2O_3.

Opaque minerals are much scarcer in the metabasites. They tend to be either pyrite or magnetite. Magnetite often shows late stage alteration.

Aragonite/Calcite

Calcite or aragonite partially altered to calcite occurs in some metabasites as interstitial grains or veins. In some cases it pseudomorphs lawsonite. No other carbonate was found in the area.

In the Devlez area only one specimen (394/3) was found to contain *pumpellyite* in a lamellar intergrowth with lawsonite.

Talc

Talc was only found in one of the analysed specimens (356) coexisting with chlorite and sodic amphibole (Tables 2 and 4).

Quartz

Quartz is the dominant phase in metacherts and is present in small amounts in many metabasites (Tables 2 and 3).

Albite

Albite is a very rare mineral. It was only found in two metabasites where it is pure albite with no detectable anorthite component.

In the blueschist facies sodic amphiboles and pyroxenes take up only trace amounts of titanium; subsequently *sphene* becomes a ubiquitous accessory mineral in metabasites. It is less common in metacherts (Table 2) where titanium enters hematite instead of forming sphene. Sphene occurs as poorly crystalline dusty brown aggregates. Rutile is not found in the area. Blueschist minerals notable in their absence in the Devlez area include stilpnomelane and deerite. The absence of these two minerals can be related to the lack of suitable iron-rich rock compositions and to the generally high oxidation states of the blueschists. However, as *stilpnomelane* is an important mineral in the more reduced blueschists, such as Franciscan metacherts, five stilpnomelane-bearing mineral assemblages were analysed: one from a meta-acidic rock 8 km south of the area shown in Fig. 1, and four Franciscan metacherts (from Healdsburg, Tiburan, Pacheco Pass, and Panoche Pass). The essential mineral assemblage in Franciscan metacherts is 'quartz + sodic amphibole + stilpnomelane + garnet + phengite + chlorite' and in the meta-acidic rock from Tavsanli 'albite + stilpnomelane + sodic amphibole + quartz + ilmenite + lawsonite'. Sodic amphiboles coexisting with stilpnomelane have compositions with $Fe^{2+}/Fe^{2+} + Mg$ ratios greater than 0.5 (Fig. 12a) characteristic of reduced mineral assemblages which recrystallized

Table 4. Compositions of minerals

	Sodic amphiboles								Sodic pyroxenes					
	357/1		643/2	182	380	381	460	473	33	471	643/2	182	381	395
	core	rim												
SiO_2	57.36	56.71	55.99	58.20	57.54	56.52	57.91	58.70	53.42	53.75	53.57	55.13	52.69	58.37
Al_2O_3	11.00	7.83	6.46	7.72	4.87	3.80	5.72	6.70	4.52	5.58	5.47	8.50	3.77	19.59
TiO_2	0.00	0.00	0.00	0.00	0.00	0.00	0.00	0.00	0.00	0.00	0.19	0.00	0.00	0.00
FeO*	10.47	15.12	16.71	11.65	16.52	23.87	15.00	8.18	17.74	13.85	14.88	18.44	22.97	7.55
MnO	0.00	0.00	0.15	0.20	0.16	0.13	0.27	0.45	0.23	0.30	0.00	0.00	0.00	0.00
MgO	9.86	8.89	8.79	11.16	10.39	6.57	10.67	14.00	4.00	5.55	4.93	0.91	1.52	0.00
CaO	1.07	0.44	0.72	0.09	0.86	0.22	0.69	0.89	8.10	13.36	9.19	1.92	4.07	0.09
Na_2O	6.72	7.23	6.97	7.76	6.84	7.46	7.22	7.26	9.16	6.36	8.81	13.13	11.56	14.38
Total	96.48	96.22	95.80	96.79	97.18	98.58	97,49	96.18	97.15	98.75	97.03	98.02	96.58	99.97

* Total iron as FeO

	Number of cations per 23 oxygens								Number of cations per 6 oxygens					
Si	7.97	8.00	7.99	8.01	8.07	8.03	8.04	8.02	2.01	2.00	2.00	2.01	2.00	2.01
Al^{iv}	0.03	0.00	0.01	0.00	0.00	0.00	0.00	0.00	0.00	0.00	0.00	0.00	0.00	0.00
Al^{vi}	1.77	1.30	1.08	1.25	0.81	0.64	0.94	1.08	0.20	0.25	0.24	0.37	0.17	0.80
Ti	0.00	0.00	0.00	0.00	0.00	0.00	0.00	0.00	0.00	0.00	0.01	0.00	0.00	0.00
Fe^{3+}	0.22	0.67	0.86	0.70	1.11	1.37	0.95	0.80	0.46	0.21	0.40	0.56	0.68	0.16
Fe^{2+}	1.00	1.11	1.14	0.64	0.83	1.47	0.79	0.13	0.10	0.22	0.07	0.00	0.05	0.06
Mn	0.00	0.00	0.02	0.02	0.02	0.02	0.03	0.05	0.01	0.01	0.00	0.00	0.00	0.00
Mg	2.04	1.87	1.87	2.29	2.17	1.39	2.21	2.85	0.22	0.31	0.28	0.05	0.09	0.00
Σ	5.03	4.95	4.97	4.90	4.94	4.89	4.92	4.92	0.99	1.00	1.00	0.98	0.99	1.02
Ca	0.16	0.07	0.11	0.01	0.13	0.03	0.10	0.13	0.33	0.54	0.37	0.08	0.17	0.00
Na	1.81	1.98	1.93	2.07	1.86	2.06	1.94	1.92	0.66	0.46	0.64	0.93	0.85	0.96
Σ	1.97	2.05	2.04	2.08	1.99	2.09	2.04	2.05	0.99	1.00	1.01	1.01	1.02	0.96
								Jd	20	25	24	37	17	80
								Ac	46	21	40	56	68	20
								Au	34	54	36	7	15	0

well within the magnetite stability field (Okay, in press). With these compositions the whole sodic amphibole field, with the exception of an area around the glaucophane end-member, can be inferred to be potentially stable in the glaucophane-lawsonite facies.

Element Partitioning

The variable ferromagnesian ratios of phengites and sodic pyroxenes within a single section and their restricted range do not allow reliable distribution coefficients between them and other minerals to be determined. Discussion on element partitioning is consequently restricted to the Fe^{2+}/Mg distribution between chlorite and sodic amphibole and Al/Fe^{3+} distribution between sodic amphibole and sodic pyroxene.

Chlorite-Sodic Amphibole

Fe^{2+}/Mg ratios for seventeen coexisting homogeneous sodic amphiboles and chlorites are shown in Fig. 9a. Thirteen of the pairs come from Devlez, 2 from Gümele (Lünel 1967), one from Mihalliçik (Çogulu 1967) and one from Panoche Pass, California. The main errors in the determination of the partition coefficient K_D arise from the uncertainty of ferric/ferrous recalculation in sodic amphibole microprobe analyses and the minor undetermined ferric ion in chlorite.

The Fe^{2+}/Mg distribution coefficient is strongly dependent on the calcium content of the sodic amphibole and ranges from 1.1 for low calcium substitution ($0.00 < Ca/Ca+Na < 0.03$) to 0.8 for increased cal-

Table 4 (Continued)

	Chlorites				Talc	Garnets					
	27	33	356	182	356	357/1	471		380	460	473
							core	rim			
SiO_2	27.75	27.68	28.77	29.17	61.28	38.14	37.85	37.87	36.99	37.25	37.57
Al_2O_3	17.58	17.56	18.52	20.39	0.00	21.99	21.31	21.38	19.74	20.77	20.19
TiO_2	0.00	0.00	0.00	0.00	0.00	0.20	0.00	0.00	0.25	0.33	0.28
FeO*	22.99	21.62	18.28	10.77	8.18	28.40	15.34	22.34	9.49	7.40	2.98
MnO	0.69	1.23	0.32	0.52	0.00	0.84	13.71	7.29	26.17	30.64	33.85
MgO	17.67	19.19	21.47	25.12	25.72	2.25	0.00	0.32	0.27	0.27	0.29
CaO	0.09	0.00	0.08	0.00	0.00	9.08	13.12	11.78	7.33	5.74	0.56
Total	86.77	87.26	87.44	86.11	95.19	100.89	101.34	100.97	100.25	102.30	101.72
Number of cations per:											
		28 oxygens			22 oxygens	8 oxygens					
Si	5.85	5.78	5.84	5.78	8.04	2.99	2.98	3.00	2.99	2.96	3.00
Al^{iv}	2.15	2.22	2.16	2.22	0.00	0.01	0.02	0.00	0.01	0.04	0.00
Al^{vi}	2.22	2.10	2.27	2.54	0.00	2.02	1.96	2.00	1.87	1.91	1.90
Fe^{3+}	–	–	–	–	–	0.00	0.04	0.00	0.13	0.09	0.10
Fe^{2+}	4.05	3.78	3.10	1.78	0.90	1.85	0.97	1.48	0.51	0.40	0.10
Ti	0.00	0.00	0.00	0.00	0.00	0.01	0.00	0.00	0.01	0.01	0.02
Mn	0.12	0.22	0.06	0.09	0.00	0.06	0.92	0.49	1.79	2.06	2.29
Mg	5.55	5.97	6.50	7.41	5.03	0.26	0.00	0.04	0.03	0.03	0.03
Ca	0.02	0.00	0.02	0.00	0.00	0.76	1.11	1.00	0.64	0.49	0.56
Total	19.97	20.06	19.95	19.84	13.97	7.98	8.00	8.01	8.00	8.00	8.00

* Total iron as FeO

Alm.	63	32	49	17	13	3
Spess.	2	31	17	60	69	76
Pyr.	9	0	1	1	1	1
Gross.	26	37	33	22	17	19

	Phengites					
	33	357/1	380	460	473	395
SiO_2	51.43	51.71	52.20	52.15	51.50	47.75
Al_2O_3	22.50	22.95	23.00	23.27	24.96	30.04
TiO_2	0.00	0.20	0.22	0.00	0.14	0.00
FeO*	4.95	3.93	4.50	4.45	2.78	3.93
MnO	0.00	0.00	0.18	0.12	0.13	0.34
MgO	3.75	3.78	3.88	3.83	3.71	0.94
CaO	0.00	0.16	0.00	0.00	0.00	0.00
Na_2O	0.00	0.00	0.00	0.00	0.00	0.00
K_2O	10.83	10.80	10.86	10.81	10.50	10.05
Total	93.45	93.52	94.84	94.64	93.72	93.05

	Number of cations per 22 oxygens					
	33	357/1	380	460	473	395
Si	7.10	7.10	7.09	7.09	6.99	6.57
Al^{iv}	0.90	0.90	0.91	0.91	1.01	1.43
Al^{vi}	2.76	2.81	2.77	2.82	2.99	3.44
Ti	0.00	0.02	0.02	0.00	0.01	0.00
Fe^{2+}	0.57	0.45	0.51	0.51	0.32	0.45
Mn	0.00	0.00	0.02	0.01	0.02	0.04
Mg	0.77	0.77	0.79	0.78	0.75	0.19
Σ	4.10	4.06	4.11	4.12	4.09	4.12
Ca	0.00	0.02	0.00	0.00	0.00	0.00
Na	0.00	0.00	0.00	0.00	0.00	0.00
K	1.91	1.89	1.88	1.87	1.82	1.76
Total	14.01	13.97	13.99	13.99	13.91	13.88

* Total iron as FeO

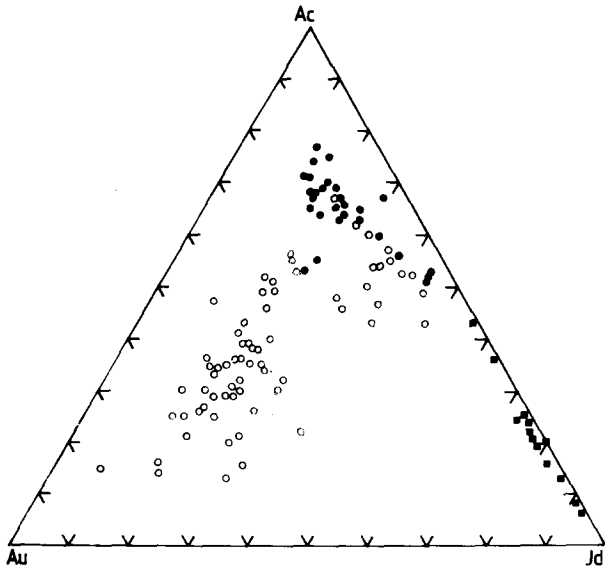

Fig. 4. Compositions of sodic pyroxenes plotted on acmite-jadeite-augite diagram. Sodic pyroxenes from metacherts, *filled circles*; from metabasites, *open circles*; from metakeratophyres, *filled squares*

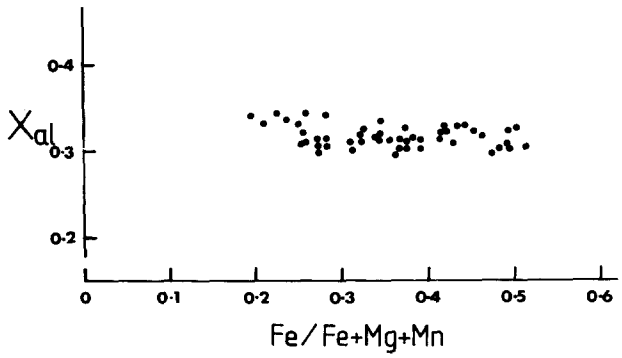

Fig. 5. Composition of chlorites from Northeast Tavşanlı plotted in terms of their Fe/(Fe+Mg+Mn) and Al/(Al+Fe+Mg+Mn) ratios

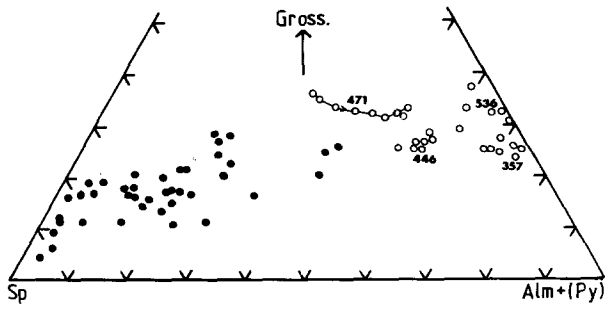

Fig. 6. Garnet compositions plotted on spessartine-grossular-(almandine+pyrope) diagram; all pyrope contents below 9%. Garnets from metacherts, *filled circles*; from metabasites, *open circles*

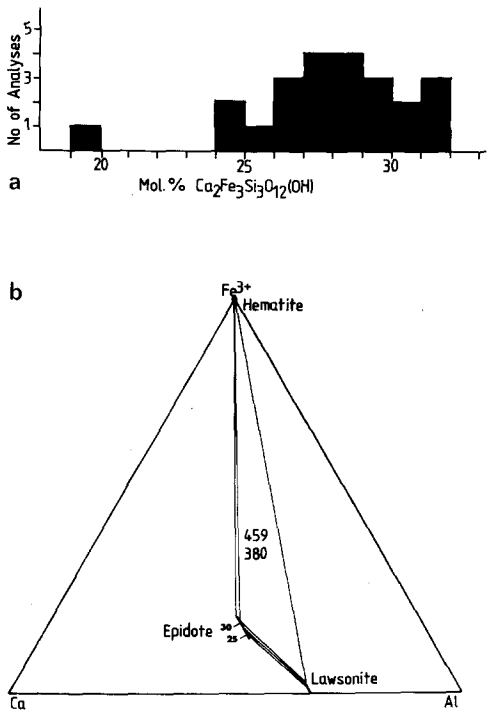

Fig. 7. **a** Compositions of 23 epidotes from 7 blueschists plotted in terms of their pistacite components. **b** The compositionally invariant epidote-lawsonite-hematite assemblage in the $Ca-Fe^{3+}-Al$ system from two metacherts (380 and 459)

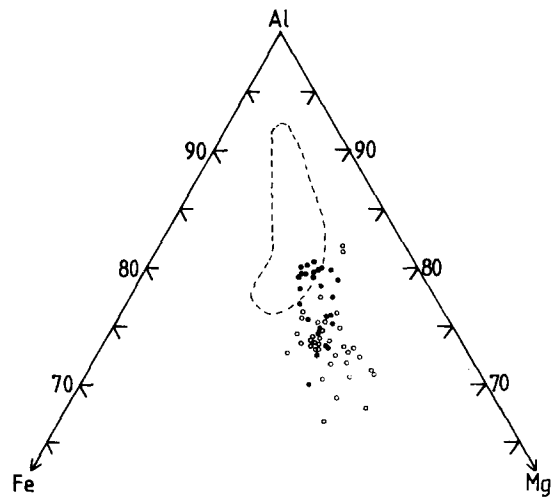

Fig. 8. Phengite compositions plotted on Al–Fe–Mg diagram. Phengites from metacherts, *filled circles*; from metabasites, *open circles*. Compositional field of phengites from Eastern Otago greenschists (Brown 1967) are shown by *dashed lines*

cium substitution ($0.03 < X_{Ca} < 0.10$) in sodic amphibole. A decrease in the partition coefficient, with increasing calcium content in sodic amphibole, is to be expected as the K_D for actinolite/chlorite pairs is 0.58 (Kawachi 1975; Coombs et al. 1976).

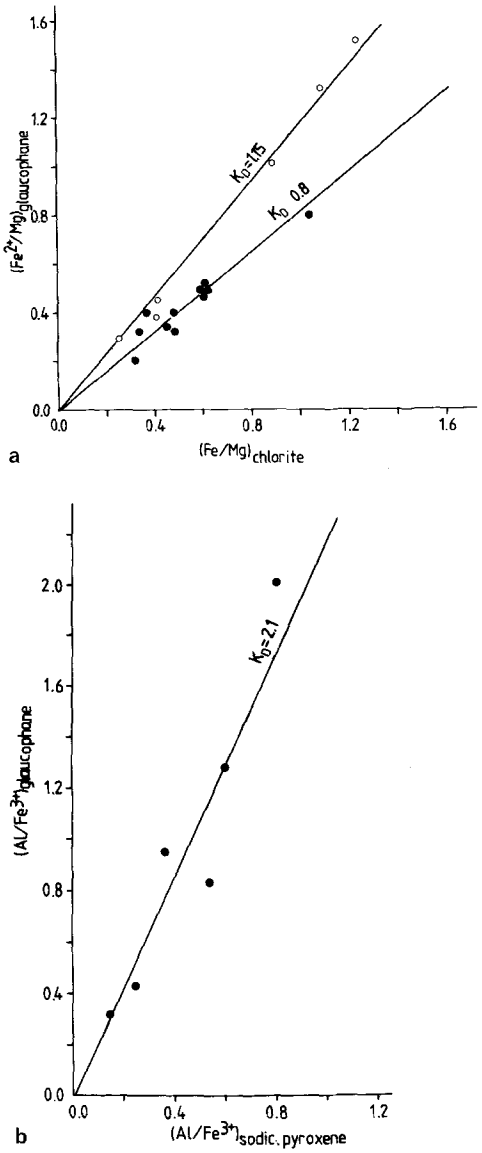

Fig. 9.a Fe^{2+}/Mg ratios in coexisting sodic amphibole and chlorite, where Fe* = total Fe. Sodic amphiboles with $X_{Ca} < 0.03$, *open circles*; sodic amphiboles with $0.03 < X_{Ca} < 0.1$, *filled circles*. **b** Al/Fe^{3+} ratios in coexisting sodic amphibole and sodic pyroxene

Sodic Amphibole-Sodic Pyroxene

Most sodic pyroxenes and amphiboles from the Tavsanli area show zoning in their Al and Fe^{3+} components. Six relatively homogeneous sodic amphibole-sodic pyroxene pairs are shown in Fig. 9b; five come from Devlez, one from Mihallicik. The partition coefficient K_D of 2.1 is quite different from 0.8 found by Onuki and Ernst (1969).

The Composition of the Fluid Phase and the Status of CO_2

The abundance of hydrous blueschist minerals, such as lawsonite and/or sodic amphibole, in the initially anhydrous basic igneous rocks is prima facie evidence for the presence of fluid phase during the regional metamorphism. The lack of graphite in the blueschists suggests that the two main components of the fluid phase were H_2O and CO_2. The common occurrence of lawsonite-quartz and phengite-sphene subassemblages indicate that the fluid was dominated by H_2O ($X_{CO_2} < 0.02$, Hunt and Kerrick 1977 p. 286; Nitsch 1972).

In the phase relations analysis, CO_2 can be regarded either as as mobile component like H_2O, or as an inert component like O_2 (Zen 1974). In the present study CO_2 is regarded as an inert component (like TiO_2), and consequently calcite (and aragonite) is omitted from the phase relation analysis as an indifferent phase (like sphene or phengite). The reasons for doing this are:

1. In the Tavsanli area metabasites occasionally contain minor amounts of calcite, whereas calcite is lacking in all studied metacherts. This difference in the CO_2 content between the two major rock types is most probably a primary pre-metamorphic feature. Spilites, the most likely protoliths of metabasites, might well have contained small amounts of CO_2 stored in calcite, which was preserved through the metamorphism;

2. Most of the calcite-bearing metabasites contain the assemblage lawsonite + calcite + quartz (Table 2) which is a buffer for CO_2 by the reaction: lawsonite + CO_2 = calcite + quartz + pyrophyllite + H_2O.

Under most metamorphic conditions pyrophyllite is probably not stable relative to potassium-mica. It is unlikely, that this buffered assemblage could be maintained at an externally controlled chemical potential of CO_2; rather it suggests fCO_2 was buffered at very low values by the mineral assemblage.

3. No differences either in the mineral assemblage or mineral compositions can be detected between calcite-bearing and calcite-free rocks.

Approach to Equilibrium

The underlying principle of the phase relations analysis is the assumption that equilibrium has been achieved between coexisting minerals at a single value of $P-T-X$. This assumption is not strictly valid especially for the lower grades of metamorphism such as the blueschist facies, where mineral zoning is common, relict minerals are present and former mineral

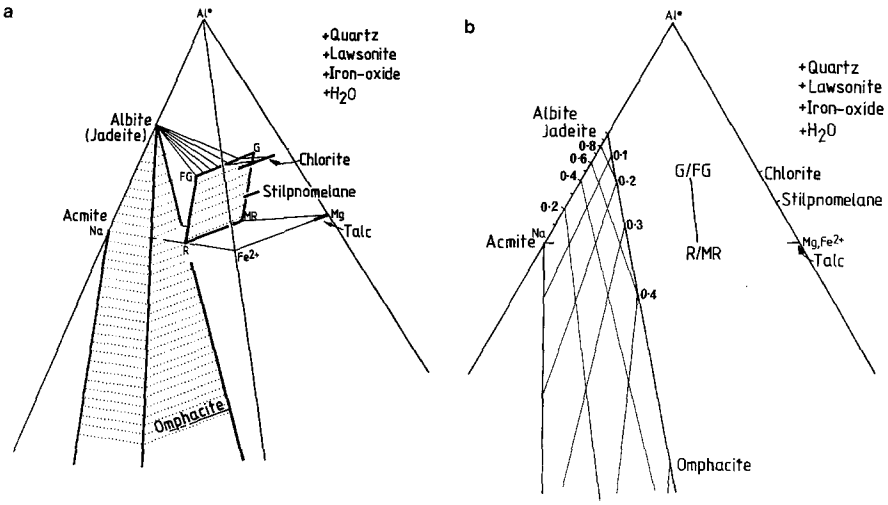

Fig. 10. a NAFM projection of mineral compositions from quartz, lawsonite and iron-oxide (hematite) onto the tetrahedra $Na-Al^*-Fe^{2+}-Mg$. Only some of the tie lines are indicated. $Al^*=(Al-2Ca)$. **b** Projection of mineral compositions from quartz, lawsonite, H_2O and iron-oxide (hematite) onto the plane $Na-Al^*-(Fe^{2+}, Mg)$. The jadeite and augite contents of sodic pyroxenes are also indicated. $Al^*=(Al-2Ca)$

assemblages may be recognizable. However, the establishment of the ideal phase compatibilities at different $P-T-X$ values is important in understanding the evolution of mineral assemblages through metamorphism. Phase relations established from equilibrated mineral assemblages can then be used to understand the nature of 'frozen reactions' and zoning in minerals.

Metamorphic minerals are assumed to have reached equilibrium in equigranular, schistose metacherts (see Fig. 2) and metabasites. Rocks with reaction textures involving replacement of sodic pyroxene by sodic amphibole are interpreted to be in disequilibrium.

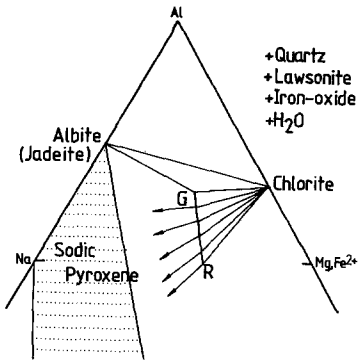

Fig. 11. Model phase relations in the glaucophane-lawsonite facies for moderate $Fe^{2+}/Fe^{2+}+Mg$ values (0.30–0.50) in the rock, shown on a NAF diagram. Sodic pyroxene field is *stippled*

Phase Relations

The minerals considered in this study can be represented to a first approximation in the system $Na_2O-K_2O-CaO-MgO-FeO-MnO-Fe_2O_3-Al_2O_3-TiO_2-SiO_2-H_2O$. K_2O, MnO and TiO_2 are assumed to affect only the formation of the phases phengite, spessartine and sphene respectively. By considering quartz-bearing assemblages SiO_2 is regarded as an excess component, and H_2O is taken as a perfectly mobile component. The chemographic relationships are further simplified by projecting from lawsonite for CaO and from hematite for Fe_2O_3 into the system $Na_2O-MgO-FeO-Al_2O_3$ (NAFM). All projections are made from hematite although part of the sodic amphibole field, as well as almandine and stilpnomelane are only stable with magnetite. However, projecting from magnetite will only slightly alter the coordinates of sodic pyroxenes and amphiboles in the NAFM system but will not have any effect on the topology. The algebraic procedure used for projecting phases is that given by Greenwood (1975).

Phase relations in the glaucophane-lawsonite facies between the minerals sodic amphibole, chlorite, albite, sodic pyroxene, almandine, stilpnomelane and talc are shown in Fig. 10a. In the NAFM diagram sodic pyroxenes project into an open ended 'beak' shaped volume with the calcic end-members plotting below the $Al-Fe^{2+}-Mg$ plane. The positions of different sodic pyroxene end-members are shown in a NAF triangular diagram (Fig. 10b) where Fe^{2+} and Mg are treated as a single component. The advantage of the NAF diagram lies in the precision with which actual sodic pyroxene and sodic amphibole compositions can be plotted.

Figure 11 shows an NAF diagram for moderate $Fe^{2+}/Fe^{2+}+Mg$ values (0.3–0.5), where chlorite is the stable ferromagnesian phase. Here, the important, compositionally invariant assemblage is albite (jadeite)-chlorite-sodic amphibole plus the projected phases. Such assemblages are found in Northwest Turkey, in New Caledonia (Black 1973, p. 224) and in many other areas.

At lower $Fe^{2+}/Fe^{2+}+Mg$ values (<0.25) talc, and at higher $Fe^{2+}/Fe^{2+}+Mg$ values (>0.55) stillp-

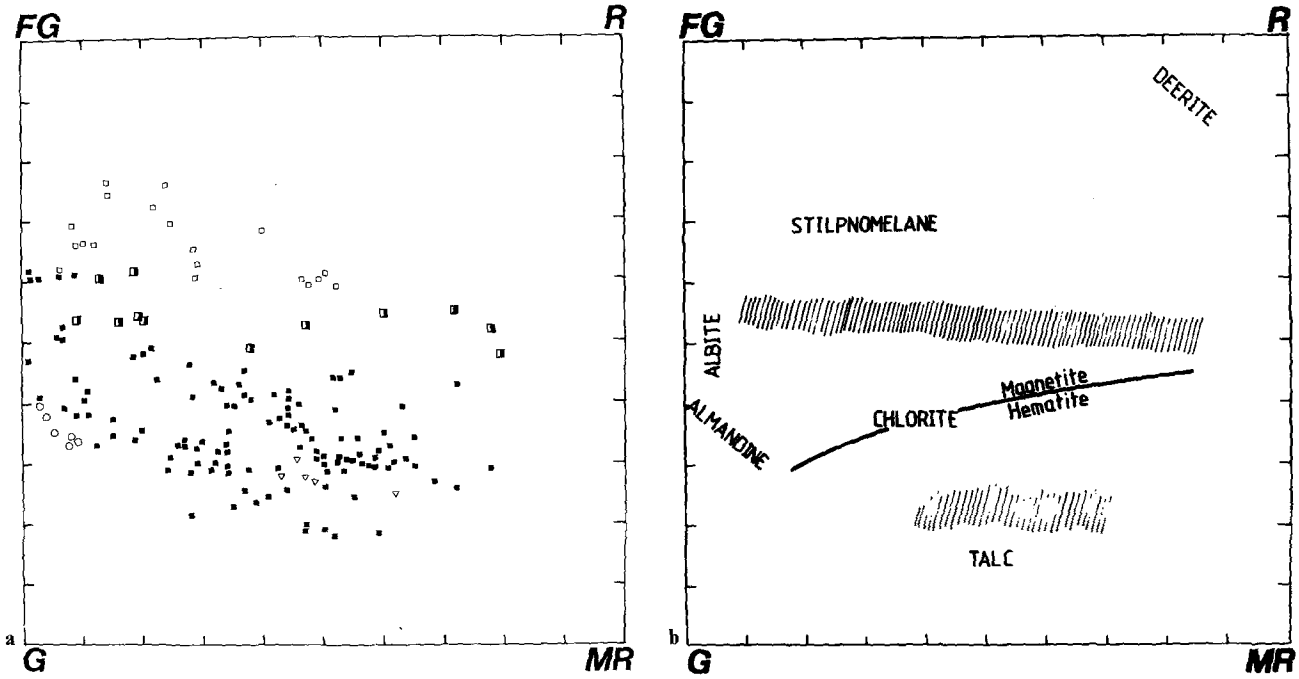

Fig. 12. a Sodic amphibole composition in relation to the mineral assemblage. Sodic amphibole with chlorite, *solid squares*; with stilpnomelane, *open squares*; with chlorite and stilpnomelane, *half-filled squares*; with almandine, *open circles*; with talc and chlorite, *open triangles*. **b** Phase relations of sodic amphibole in the glaucophane-lawsonite facies. Sodic amphibole compositions which may coexist with two ferromagnesian minerals are ruled. Iron-oxides most probably can coexist with all sodic amphibole compositions. Albite is restricted to glaucophane-ferroglaucophane solid solution

nomelane are the stable ferromagnesian minerals coexisting with sodic amphibole. The change from one ferromagnesian mineral to another occurs at approximately constant $Fe^{2+}/Fe^{2+}+Mg$ and therefore cannot be successfully illustrated on the NAF diagram.

A peculiar problem in the Devlez area is the presence of almandine garnets with 25%–35% grossular component coexisting with Al-rich amphiboles. When projected from lawsonite for Ca on the NAF plane, the garnets plot near the Fe^{2+}, Mg (F) apex; since chlorite coexists with comparatively Al-poor sodic amphibole, garnet-amphibole and chlorite-amphibole tie lines cross.

There is no textural evidence for any disequilibrium between coexisting lawsonite and garnet. Furthermore garnets from the Cazadero area metabasites, coexisting with lawsonite and aluminous sodic amphibole (Coleman and Papike 1968, p. 111), have similar grossular components (25%–30%; Lee et al. 1963, p. 472). It seems that the blueschists of the Devlez area recrystallized at the critical $P-T$ conditions corresponding to the chlorite-garnet transition.

Instability of Sodic Pyroxene + Chlorite

Sodic pyroxenes contain proportionately higher amounts of Na+Ca than sodic amphiboles, consequently they are restricted to the sodium-rich corner of the NAFM diagram. They are separated from the ferromagnesian minerals by the intervening sodic amphibole compositional field and albite-sodic amphibole tie lines (Fig. 10a). Thus acmite- and jadeite-rich sodic pyroxenes cannot coexist with ferromagnesian minerals, instead sodic amphibole is the stable phase. Obviously sodic pyroxene can coexist stably with sodic amphibole in assemblages free of any ferromagnesian minerals, as in the sodium-rich metachert 381 (Table 3).

The coexistence of sodic pyroxene with chlorite and sodic amphibole in many blueschist metabasites from the Devlez area is due to an imcomplete prograde sodic amphibole producing reaction involving sodic pyroxene and chlorite (Okay in preparation).

The Composition of Sodic Amphibole in Relation to Mineral Assemblage

All phases in the NAFM system have tielines extending to the sodic amphibole field; therefore the compositional field of sodic amphiboles can be used as a plane on which other phases are projected in terms of actual sodic amphibole compositions (Brown 1974).

In quartz-bearing rocks, sodic amphibole can be

regarded as consisting of five major components (Na_2O, MgO, FeO, Al_2O_3, Fe_2O_3), consequently any three phases in the NAFM diagram plus iron-oxide should coexist with a single composition of sodic amphibole. Sodic amphibole coexisting with two other phases in the NAFM diagram plus iron-oxide should be compositionally univariant; the composition should vary along a line on the Miyashiro diagram.

In Fig. 12a sodic amphiboles are shown in terms of coexisting minerals; the figure includes sodic amphiboles from Gümele (Lünel 1967) and from stilpnomelane-bearing Franciscan metacherts, as well as sodic amphiboles from the Devlez area. The sodic amphibole compositional field is divided into four major regions each associated with one of the following ferromagnesian minerals: chlorite, almandine, talc and stilpnomelane; a fifth 'deerite' region is present around the riebeckite end-member (Muir Wood 1977, p. 256).

Spessartine-rich garnets are stable with all sodic amphibole compositions as an extra Mn-bearing phase; only almandine with negligible spessartine component is restricted to glaucophane (s.l.) bearing assemblages (357/1 and 536). However, as discussed earlier, almandine might represent a higher grade of metamorphism. Sodic pyroxenes are not shown as they do not coexist stably with the other ferromagnesian minerals, lying on the opposite side of the sodic amphibole compositional field (Fig. 10a).

The position of univariant lines on the sodic amphibole field will depend to some extent on the calcium content of the sodic amphibole which has an important effect on the Fe^{2+}/Mg partitioning between sodic amphibole and other minerals. Variations in the calcium content of sodic amphibole and uncertainties in the ferric/ferrous recalculation will result in compositional bands, rather than lines, on the sodic amphibole field, marking the coexistence of two ferromagnesian minerals (Fig. 12b).

Brown (1974) first related sodic amphibole composition to coexisting minerals in the blueschists from Shuksan. The main difference between the diagram here and Brown's diagram (1974, Fig. 11) is in the treatment of iron-oxides; as many of Brown's amphibole assemblages lacked iron-oxides, he assumed that iron-oxides were not stable with ferroglaucophane and glaucophane compositions. However, sodic amphibole compositions from Northwest Turkey demonstrate that this is not the case (Okay, in press); the absence of iron-oxides in some assemblages is possibly due to low amounts of ferric ion in the rock giving increased compositional freedom.

Acknowledgements. I thank S.O. Agrell, E.H. Brown, G.T.R. Droop, J.G. Spray, and R. Muir Wood for reviewing the manuscript. Probe facilities were provided by the Department of Mineralogy and Petrology in Cambridge. This work was carried out while in receipt of a grant from the Mineral Research and Exploration Institute of Turkey (M.T.A.), which is gratefully acknowledged.

References

Black, P.M.: Mineralogy of New Caledonian metamorphic rocks I. Garnets from the Ouegoa district. Contrib. Mineral. Petrol. **38**, 221–235 (1973)

Black, P.M.: Mineralogy of New Caledonian metamorphic rocks IV. Sheet silicates from the Ouegoa district. Contrib. Mineral. Petrol. **49**, 269–284 (1975)

Brinkmann, R.: Mesozoic troughs and crustal structure in Anatolia. Bull. Geol. Soc. Am. **83**, 819–826 (1972)

Brown, E.H.: The greenschist facies in part of Eastern Otago, New Zealand. Contrib. Mineral. Petrol. **14**, 259–292 (1967)

Brown, E.H.: Comparison of the mineralogy and phase relations of blueschists from the North Cascades, Washington and greenschists from Otago, New Zealand. Bull. Geol. Soc. Am. **85**, 333–344 (1974)

Çoğulu, E.: Etude pétrographique de la région de Mihalliççik (Turquie). Schweiz. Mineral. Petrogr. Mitt. **47**, 683–824 (1967)

Çoğulu, E., Krummenacher, D.: Problèmes géochronométriques dans la partie NW de l'Anatolie Centre (Turquie). Schweiz. Mineral. Petrogr. Mitt. **47**, 825–831 (1967)

Coleman, R.G., Lee, D.E.: Glaucophane-bearing metamorphic types of the Cazedoro area, California. J. Petrol. **4**, 260–301 (1963)

Coleman, R.G., Papike, J.J.: Alkali amphiboles from the blueschists of Cazadero, California. J. Petrol. **9**, 105–122 (1968)

Coombs, D.S., Nakamura, Y., Vuagnat, M.: Pumpellyite-actinolite facies schists of the Taveyanne Formation near Loeche, Valais, Switzerland. J. Petrol. **17**, 440–471 (1976)

Cooper, A.F.: Progressive metamorphism of metabasic rocks from the Haast Schist Group of Southern New Zealand. J. Petrol. **13**, 457–492 (1972)

Ernst, W.G., Seki, Y., Onuki, H., Gilbert, M.C.: Comparative study of low-grade metamorphism in the California Coast Ranges and the outer metamorphic belt of Japan. Geol. Soc. Am., Mem. **124**, 259 (1970)

Essene, E.J., Fyfe, W.S.: Omphacite in Californian metamorphic rocks. Contrib. Mineral. Petrol. **15**, 1–23 (1967)

Greenwood, H.J.: Thermodynamically valid projections of extensive phase relationships. Am. Mineral. **60**, 1–8 (1975)

Hsu, L.C.: Selected phase relationships in the system Al–Mn–Fe–Si–O; a model for garnet equilibria. J. Petrol. **9**, 40–83 (1968)

Hunt, J.A., Kerrick, D.M.: The stability of sphene: experimental redetermination and geological implications. Geochim. Cosmochim. Acta **41**, 279–288 (1977)

Kaaden, G.v.d.: The significance and distribution of glaucophane rocks in Turkey. Bull. Miner. Res. Explor. Inst. Turk. **67**, 37–67 (1966)

Kawachi, Y.: Pumpellyite-actinolite and contiguous facies metamorphism in part of upper Wakatipu district, South Island, New Zealand. N.Z.J. Geol. Geophys. **18**, 401–441 (1975)

Kaya, O.: Aufbau und Geschichte einer anatolischen Opiolith-Zone. Z. Deutsch. Geol. Ges. **123**, 491–501 (1972)

Kaya, O.: Outlines of the ophiolite question in the Tavsanli region (in Turkish). Bull. Geol. Soc. Turk. **15**, 26–108 (1972)

Lee, D.E., Coleman, R.G., Erd, R.C.: Garnet types from the Cazadero area, California. J. Petrol. **4**, 460–492 (1963)

Lünel, T.: Geology of Sübren-Karaalan area, Eskişehir county

(Turkey). Ph. D Thesis (unpublished), University of Bristol 1967

Maden Tetkik ve Arama Enst.: Geological maps of Turkey; Ankara sheet 1963; Istanbul, Zonguldak, İzmir sheets. Ankara: M.T.A. Publications 1964

Miyashiro, A.: The chemistry, optics and genesis of the alkali amphiboles. J. Fac. Sci., Univ. Tokyo, Sect. 2 **11**, 57–83 (1957)

Muir Wood, R.: The iron-rich blueschist facies minerals: I Deerite. Mineral. Mag. **43**, 251–259 (1979)

Nitsch, K.H.: Das $P-T-X_{CO_2}$ Stabilitatsfield von Lawsonit. Contrib. Mineral. Petrol. **34**, 116–134 (1972)

Okay, A.I.: Sodic pyroxenes from metabasites in the eastern Mediterranean. Contrib. Mineral. Petrol. **68**, 7–11 (1978)

Okay, A.I.: Sodic amphiboles as oxygen fugacity indicators in metamorphism. J. Geol. (in press)

Onuki, H., Ernst, W.G.: Coexisting sodic amphiboles and sodic pyroxenes from blueschist facies metamorphic rocks. Mineral. Soc. Am., Spec. Pap. **2**, 241–250 (1969)

Roever, E.W.F., de: Blue amphibole-albite-chlorite assemblages from Fuscaldo (Southern Italy) and the role of glaucophane in metamorphism. Contrib. Mineral. Petrol. **58**, 221–234 (1976)

Statham, P.J.: A comparative study of techniques for quantitative analysis of the X-ray spectra obtained with a Si(Li) detector. X-Ray Spectrom. **5**, 16–28 (1976)

Sweatman, R.R., Long, J.V.P.: Quantitative electron probe microanalysis of rock forming minerals. J. Petrol. **10**, 332–379 (1969)

Zen, E-An.: Prehnite and pumpellyite bearing mineral assemblages west side of the Appalachian metamorphic belt, Pennsylvinia to Newfoundland. J. Petrol. **15**, 197–242 (1974)

Received December 21, 1979; Accepted February 7, 1980